

# ERROR AND SYMMETRY ANALYSIS OF MISNER'S ALGORITHM FOR SPHERICAL HARMONIC DECOMPOSITION ON A CUBIC GRID

DAVID R. FISKE\*

**Abstract.** Computing spherical harmonic decompositions is a ubiquitous technique that arises in a wide variety of disciplines and a large number of scientific codes. Because spherical harmonics are defined by integrals over spheres, however, one must perform some sort of interpolation in order to compute them when data is stored on a cubic lattice. Misner (2004, *Class. Quant. Grav.*, **21**, S243) presented a novel algorithm for computing the spherical harmonic components of data represented on a cubic grid, which has been found in real applications to be both efficient and robust to the presence of mesh refinement boundaries. At the same time, however, practical applications of the algorithm require knowledge of how the truncation errors of the algorithm depend on the various parameters in the algorithm. Based on analytic arguments and experience using the algorithm in real numerical simulations, I explore these dependencies and provide a rule of thumb for choosing the parameters based on the truncation errors of the underlying data. I also demonstrate that symmetries in the spherical harmonics themselves allow for an even more efficient implementation of the algorithm than was suggested by Misner in his original paper.

**1. Introduction.** Spherical harmonic decomposition is a ubiquitous mathematical technique that arises in a wide variety of disciplines. It is no surprise, therefore, that it also arises in an equally varied range of scientific computing applications. It plays a key role, for example, in currently active algorithms, for determining compatible docking configurations of organic molecules [5, 12], modeling atmospheric and oceanic flows [1, 9, 11], representing human population density on the surface of the earth [10], analyzing experimental data regarding turbulent magnetohydrodynamic flows [8], and analyzing numerical simulations of gravitational radiation emitted from the collisions of black holes [2, 3].

In numerical calculations structured on a cubic grid, however, extracting spherical harmonic components can be non-trivial since the spherical harmonic components  $\Phi_{lm}$  of a function  $\Phi$  are defined by integrals over spheres

$$\Phi_{lm}(t, r) = \oint \bar{Y}_{lm}(\theta, \phi) \Phi(t, r, \theta, \phi) d\Omega \quad (1.1)$$

that have few if any intersections with the cubic lattice. Misner recently presented a particularly nice approach to solving this problem, which does not require explicit interpolations from the cubic grid to an integration sphere [6]. The mathematical grounding of the algorithm is laid out completely in Ref. [6], but the original reference does not provide any detailed analysis of the numerical errors incurred by the approximation. In practical applications, such error estimates have been found essential for choosing the parameters of the algorithm and for understanding the results of simulations [2, 3]. In addition, making use of the symmetries of the spherical harmonics allows certain simplifications of the algorithm as applied to generic data and, especially, as applied to data with explicit grid symmetries when only the independent portion of the data is evolved.

It should be noted that although, in my discussion, I will always speak of spherical harmonics in their usual sense, everything in this paper is also true for spin-weighted

---

\*Department of Physics, University of Maryland, College Park, MD 20742, and Laboratory for Gravitational Astrophysics, NASA Goddard Space Flight Center, Greenbelt, MD 20771, Current Address: Intelligent Systems Division, Decisive Analytics Corporation, 1235 South Clark Street, Arlington, VA 22202

spherical harmonics (see Refs. [4, 7] for definitions) except for Section 5; spin-weighted spherical harmonics do not generally have the simple symmetries that the (usual) scalar spherical harmonics have. Note also that I follow Misner in treating only the case of uniform grids, although this method was successfully applied to non-uniform grids using fixed mesh refinement. For more details on applications using spin-weighted harmonics and run on non-uniform grids, see Refs. [2, 3].

The rest of the paper is organized as follows: In Section 2, I provide a brief summary of Misner algorithm in order to establish notation for the following sections. The error analysis for the algorithm is contained in Section 3, which leads directly to Section 4, where I lay out a rule of thumb for choosing the various parameters in the algorithm. In Section 5, I provide a detailed analysis of the issues associated with and simplifications resulting from various symmetries in the spherical harmonics, and how those symmetries can be exploited for data that possesses explicit symmetries.

**2. Methodology.** In this section I outline in some detail the steps of the Misner algorithm, although I do not provide a full derivation. (See Ref. [6] for the derivation.) The purpose of this chapter is primarily to establish notation and conventions for the rest of the paper.

In order to begin, two definitions are need. First define a radial function

$$R_n(r; R, \Delta) = r^{-1} \sqrt{\frac{2n+1}{2\Delta}} P_n\left(\frac{r-R}{\Delta}\right) \quad (2.1)$$

in terms of the usual Legendre polynomials  $P_n$ . Here  $R$  and  $\Delta$  are parameters that will be associated with the radius at which the spherical harmonic decomposition is desired and half of the thickness of a shell centered on that radius. From this, define

$$Y_{nlm}(r, \theta, \phi) = R_n(r) Y_{lm}(\theta, \phi) \quad (2.2)$$

which form a complete, orthonormal set with respect to the inner product

$$\langle f|g \rangle = \int_S \bar{f}(x) g(x) d^3x \quad (2.3)$$

on the shell  $S = \{(r, \theta, \phi) \mid r \in [R-\Delta, R+\Delta]\}$ . Note also that, because the functions  $R_n$  form a complete set on the shell,

$$\Phi_{lm}(t, R) = \int \left[ \sum_{n=0}^{\infty} R_n(R; R, \Delta) R_n(r; R, \Delta) \right] \bar{Y}_{lm}(\theta, \phi) \Phi(r, \theta, \phi) d^3x \quad (2.4)$$

and that the term in brackets

$$\sum_{n=0}^{\infty} R_n(R; R, \Delta) R_n(r; R, \Delta) = r^{-2} \delta(R-r) \quad (2.5)$$

is a delta function.<sup>1</sup> (Compare (2.4) to (1.1).)

On a finite grid  $\Gamma$ , the inner product (2.3) will have the form

$$\langle f|g \rangle = \sum_{x \in \Gamma} \bar{f}(x) g(x) w_x \quad (2.6)$$

---

<sup>1</sup>The Dirac delta function is defined by the property that, for any function  $f$ , the integral  $\int_a^b f(y) \delta(x-y) dy$  is  $f(x)$  when  $x \in (a, b)$  and is 0 otherwise.

where each point has some weight  $w_x$ . This weight was given the form

$$w_x = \begin{cases} 0 & |r - R| > \Delta + h/2 \\ h^3 & |r - R| < \Delta - h/2 \\ (\Delta + h/2 - |R - r|)h^2 & \text{otherwise} \end{cases} \quad (2.7)$$

by Misner, where  $h$  is the grid spacing. Only cases with  $\Delta > h/2$  are considered. This means, roughly, that points entirely within the shell  $S$  are weighted by their finite volume on the numerical grid, points entirely outside of the shell  $S$  have zero weight, and points near the boundary are weighted according to the fraction of their volume inside  $S$ .<sup>2</sup>

With the numerical inner product (2.6), and letting capital Roman letters  $A = (nlm)$  represent index groups, the  $Y_A$  are no longer orthonormal. Their inner product

$$\langle Y_A | Y_B \rangle = G_{AB} = \bar{G}_{BA} \quad (2.8)$$

forms a metric for functions on the shell. Although a priori this matrix appears to be complex valued, I will show in Section 5 that it is actually real-symmetric and sparse. For now it suffices to follow Misner in denoting it as generically Hermitian. The inverse to this metric  $G^{AB}$  can be used to raise indices on functions defined on the sphere.

Making use of this new metric, and with some further analysis, the approximation for the spherical harmonic coefficients

$$\Phi_{lm}(t, R) = \sum_{x \in \Gamma} \bar{R}_{lm}(x; R) w_x \Phi(t, x) \quad (2.9)$$

follows with

$$R_{lm}(x; R) = \sum_{n=0}^N \bar{R}_n(R) Y^{nlm}(x) \quad (2.10)$$

in terms of  $Y^A = G^{BA} Y_B$ , not  $Y_A$ .

**3. Error Analysis.** In Ref. [6], Misner provides an algorithm for computing spherical harmonic components on a cubic lattice, but he does not provide any analysis of the errors involved. In a practical application of the method, such error analysis, in particular an analysis of the convergence order in grid spacing, is very valuable. For this reason, I wish to examine the issue more closely here.

To begin the analysis, note that there are three parameters in the algorithm, the grid spacing  $h$ , the width of the shell  $\Delta$ , and the number of terms in the sum over basis polynomials  $N$ . (Compare (2.4) to (2.9) and (2.10).) In the limit that  $h \rightarrow 0$  and  $N \rightarrow \infty$ , the numerical algorithm goes to the continuum theory. Note that, when  $h$  and  $N$  go to their limits, *any* value for  $\Delta$  is allowed, since (2.4) is an exact, continuum expression. For a finite value of  $N$ , however, the quality of the approximation in the radial direction is a function of both  $N$  and  $\Delta$ . Moreover, tying the value of  $\Delta$  to the grid spacing  $h$ , though not necessary from fundamental considerations, does in fact have advantages in terms of convergence behavior that will become clear below.

---

<sup>2</sup>Actually the boundary points are weighted by the fraction of their volume that would be inside  $S$  if the point were on a coordinate axis. See Ref. [6] for more details on the definition of the weights.

$N \setminus k$	0	2	4	6	8	10	12
0	1	1/3	1/5	1/7	1/9	1/11	1/13
2	1	0	-3/35	-2/21	-1/11	-12/143	-1/13
4	1	0	0	5/231	5/143	6/143	10/221
6	1	0	0	0	-7/1287	-23/2431	-70/4199
8	1	0	0	0	0	63/46189	15/4199
10	1	0	0	0	0	0	-33/96577

TABLE 3.1

The first few non-trivial values of  $c_{N,k}(1)$ , which are the coefficients of the Taylor expansion of a function integrated against  $d(x; N, 0, 1)$ . (In general,  $c_{N,k}(\Delta) = c_{N,k}(1)\Delta^k$ .) The values of  $k$  run across and the values of  $N$  run down. The fact that the first coefficient is always 1, and that, by increasing  $N$ , more of the sub-leading coefficients are 0 indicates that increasing  $N$  increases the order of convergence of the Misner algorithm (provided that  $\Delta \propto h$ ).

I first consider the behavior of the algorithm as a function of  $\Delta$  for fixed values of  $N$ . Define

$$d(x; N, R, \Delta) = \sum_{n=0}^N \frac{2n+1}{2\Delta} P_n \left( \frac{x-R}{\Delta} \right) P_n(0) \quad (3.1)$$

which is closely related to the delta function (2.5) in the limit  $N \rightarrow \infty$ . For finite  $N$ , this should approximate the delta function to some order of accuracy. To quantify this, consider the approximation

$$f(0) \approx I_N[f] \equiv \int_{-\Delta}^{\Delta} d(x; N, 0, \Delta) f(x) dx \quad (3.2)$$

for a suitably smooth test function  $f$ . In the limit that  $N \rightarrow \infty$ , this is exact. For any finite  $N$ , this expression can be analyzed by Taylor expanding the test function around the point  $x = 0$ . This gives, after rearranging terms and noting that all of the odd terms vanish by symmetry,

$$I_N[f] = \sum_{k=0}^{\infty} \frac{c_{N,2k}}{(2k)!} f^{(2k)}(0) \quad (3.3)$$

where

$$c_{N,k}(\Delta) = \int_{-\Delta}^{\Delta} x^k d(x; N, 0, \Delta) dx \quad (3.4)$$

are the coefficients of the expansion. In order to have a high order method, I need  $c_{N,0} = 1$ , and the coefficients corresponding to the next few values of  $k$  to vanish. Table 3.1 shows the first few coefficients  $c_{N,k}(1) = \Delta^{-k} c_{N,k}(\Delta)$  for even  $N$  in  $[0,10]$ . It is clear that each time  $N$  is increased, one more of the sub-leading coefficients vanishes. This means that there are error terms proportional to  $\Delta$ , and that the leading order term arises at  $\mathcal{O}(\Delta^{N+2})$ . In order to prevent this term, at high resolution, from dominating over discretization errors scaling like powers of the grid spacing, one should choose  $\Delta \propto h$ .

Additional error terms proportional the grid spacing  $h$  depend primarily on the order of accuracy in the volume integral when using the weights defined by (2.7). For

a finite volume, this weighing scheme provides an approximation that scales as  $\mathcal{O}(h)$ , but, for a region that is also scaling with  $h$ , the resulting integral scales as  $\mathcal{O}(h^2)$ . This provides additional motivation for choosing  $\Delta \propto h$  since most applications will require at least second order accuracy.

For higher than second order accuracy, a new scheme for computing the volume integrals is needed, but the rest of the analysis here holds true. Given such a scheme, the analysis here shows how to choose the remaining parameters to ensure that numerical errors scale like any desired power of the grid spacing.

**4. Choosing the parameters.** In practice, the grid spacing parameter  $h$  is usually chosen to resolve the sources without exceeding the physical limits of the computer. I would not expect, in general, that the grid spacing would be chosen based on the needs of this algorithm. For that reason, let me assume now that  $h$  is chosen, and discuss how to choose the remaining parameters  $N$  and  $\Delta$ . In this section I will discuss some of the theoretical issues that should be considered when choosing the parameters, leading to a rule of thumb that is valid based on this analysis and my experience with the algorithm.

The error analysis of Section 3 implies that for fixed  $\Delta$ , increasing the value of  $N$  decreases the error term. It also implies that for fixed  $N$ , increasing the value of  $\Delta$  increases the error term. This suggests taking  $\Delta$  as small as possible, and  $N$  as large as possible to make the error term as small as possible. This must be balanced, however, against practical limitations. Certainly the shell thickness  $\Delta$  needs to be large enough so that there are some grid points within the shell, otherwise the whole procedure is undefined. For fixed  $N$ , a stronger restriction requires that the Legendre polynomial  $P_N$  can be resolved over the shell. Without this condition, there would seem to be no benefit to taking higher values of  $N$ . Getting higher accuracy in practice requires finding a proper balance between choosing  $\Delta$  small and  $N$  large.

In making this balance, however, one must keep in mind that the error in the method is partially determined by the weighting scheme (2.7), which is only second order accurate in the grid spacing. I am, in addition, going to choose  $\Delta \propto h$  for reasons described above. This already suggests that taking  $N$  larger than two is pointless, since choosing  $N = 2$  already makes the piece of the error that is proportional to  $\Delta$  scale like  $\mathcal{O}(\Delta^4)$  (cf. Table 3.1), meaning that it will be an error term of sub-leading order in grid spacing. But once this term is of sub-leading order, it is much less important how large I choose  $\Delta$ , provided that I still choose it proportional to the grid spacing. I therefore adopt the following

**Rule of Thumb:** Choose  $N$  just large enough to ensure that the error term proportional to  $\Delta$  is an error term of sub-leading order in grid spacing. Choose  $\Delta$  just large enough to safely resolve  $P_N$  on the shell.

With this rule of thumb, and the second order accurate weighting scheme (2.7), I found the choices  $N = 2$  and  $\Delta = 3h/4$  completely satisfactory for a second order accurate code. Note that this corresponds to Misner's choice of  $\Delta$  in Ref. [6]. With  $N = 2$  I found that larger values of  $\Delta$  are also acceptable. Numerical results justifying these estimates appear in Ref. [2].

This is illustrated in Figure 4.1, which shows the errors in a test function as compared to an analytic solution. (The physical problem is the propagation of a linear gravitational wave through a mesh refined grid, as described in Refs. [2, 3].) It is clear from the figure that choosing  $N$  large enough makes a dramatic impact on the truncation error, whereas the exact value of  $\Delta$  for fixed  $N$  is less important. In

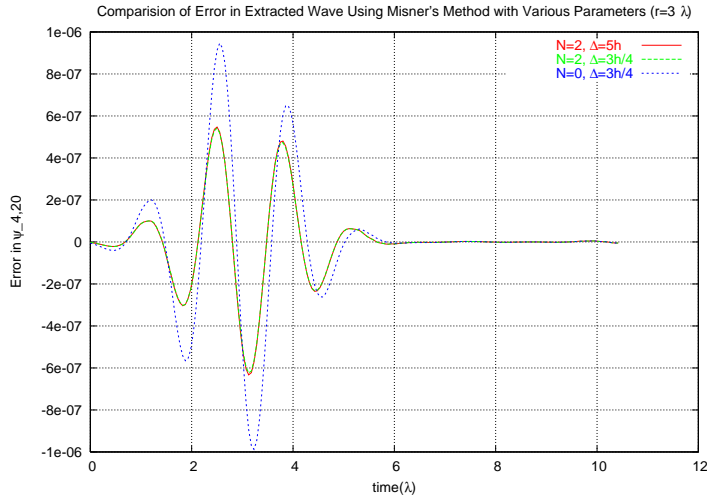


FIG. 4.1. A comparison of numerical results as a function of parameters. The lines show errors in a numerical solution as compared to an analytic solution for a sample problem. When  $N = 2$  the errors are smaller than when  $N = 0$ , consistent with the fact that the errors scale like the square of grid spacing for  $N = 2$  and only like the grid spacing for  $N = 0$ . For fixed  $N$ , the size of  $\Delta$  is fairly unimportant.

this test case, the underlying simulation was only second order accurate, so there is no benefit from choosing  $N > 2$ .

**5. Symmetry issues.** There are two points of interest related to this method of spherical harmonic decomposition and symmetries. The first was mentioned briefly in Section 2, namely that symmetry causes the metric  $G_{AB}$  to be real and sparse. The second deals with implementing the method for grids in which explicit symmetries are enforced on grid functions in order to reduce the computational load of the simulation. In these cases, in which data is not evolved over a whole extraction sphere, additional analysis is required to demonstrate that the method is well defined and to understand how to most efficiently implement it. The primary result on this second topic is that the adjoint harmonics  $Y^A$  of (2.10) have the same symmetries under reflection as the original spherical harmonics  $Y_A$ .

Consider first the implications of symmetry on the metric  $G_{AB}$ . The symmetries of the spherical harmonics, summarized in Table 5.1, cause the imaginary part of all terms in the integral (2.8) to cancel in pairs of points on the sphere related by reflections through coordinate planes. The reason is that each of the four signs  $(+1, (-1)^m, (-1)^l, \text{ and } (-1)^{l+m})$  appears twice in Table 5.1, once for a term that is complex conjugated and once for a term that is not. The matrix is also sparse. By similar reasoning, for certain values of  $l$  and  $m$ , the terms in the integral (2.8) can cancel in sets of four. Both of these facts can be seen at once through a simple calculation. The idea is to break the integral into parts using the second and third columns of Table 5.1, and then to simplify using the last two columns. Considering first just the

Planes	$\theta$	$\phi$	Sign	Conjugate
None	$\theta$	$\phi$	+1	no
$x$	$\theta$	$\pi - \phi$	$(-1)^m$	yes
$y$	$\theta$	$-\phi$	+1	yes
$z$	$\pi - \theta$	$\phi$	$(-1)^{l+m}$	no
$xy$	$\theta$	$\pi + \phi$	$(-1)^m$	no
$xz$	$\pi - \theta$	$\pi - \phi$	$(-1)^l$	yes
$yz$	$\pi - \theta$	$-\phi$	$(-1)^{l+m}$	yes
$xyz$	$\pi - \theta$	$\pi + \phi$	$(-1)^l$	no

TABLE 5.1

The table shows how the arguments of spherical harmonics transform under reflections through various Cartesian planes. The first column indicates which coordinates have their signs inverted, while the second and third columns give the new angular arguments to the spherical harmonic  $Y_{lm}$ . Alternatively, the fourth and fifth column show, respectively, the overall sign in front of and whether or not to complex conjugate the given spherical harmonic with the original angular arguments. The second row, for example, says that  $Y_{lm}(-x, y, z) = Y_{lm}(\theta, \pi - \phi) = (-1)^m Y_{lm}(\theta, \phi)$ , where  $(\theta, \phi)$  are the angular coordinates of the point  $(x, y, z)$ . Note that this table differs slightly from that in Ref. [2]. The table here is correct.

symmetries under reflection through the  $xy$ -plane and recalling the definition (2.8),

$$G_{AB} = \oint \bar{Y}_{l_1 m_1}(\theta, \phi) Y_{l_2 m_2}(\theta, \phi) d\Omega \quad (5.1a)$$

$$\begin{aligned} &= \int_0^{2\pi} \int_0^{\pi/2} \bar{Y}_{l_1 m_1}(\theta, \phi) Y_{l_2 m_2}(\theta, \phi) d\Omega \\ &\quad + \int_0^{2\pi} \int_0^{\pi/2} \bar{Y}_{l_1 m_1}(\pi - \theta, \phi) Y_{l_2 m_2}(\pi - \theta, \phi) d\Omega \end{aligned} \quad (5.1b)$$

$$= [1 + (-1)^{l_1+l_2}] \int_0^{2\pi} \int_0^{\pi/2} \bar{Y}_{l_1 m_1}(\theta, \phi) Y_{l_2 m_2}(\theta, \phi) d\Omega. \quad (5.1c)$$

(I have suppressed the radial functions since they play no role here.) Repeating the procedure for reflections through the  $xz$ - and  $yz$ -planes shows that

$$G_{AB} = 2\sigma_{m_1+m_2, l_1+l_2} \int_0^{2\pi} \int_0^{\pi/2} \text{Re} \{ \bar{Y}_{l_1 m_1}(\theta, \phi) Y_{l_2 m_2}(\theta, \phi) \} d\Omega \quad (5.2)$$

where

$$\sigma_{m_1+m_2, l_1+l_2} \equiv 1 + (-1)^{m_1+m_2} + (-1)^{l_1+l_2} + (-1)^{m_1+m_2+l_1+l_2}. \quad (5.3)$$

This proves that the matrix is real. In addition, the matrix element is zero by symmetry whenever

$$\sigma_{m_1+m_2, l_1+l_2} = 0 \quad (5.4)$$

which is true for 56 of the 81 matrix elements that exist when considering a fixed value of  $n$  and all values of  $l$  and  $m$  for  $l \leq 2$ . Of the remaining 25 matrix elements, 9, of course, are the diagonal elements that go to unity in the continuum limit. The exact break-down of which such elements must be zero by symmetry is summarized in Table 5.2. Knowing that the matrix is real-symmetric and sparse allows for a more

$m_1 + m_2$	$l_1 + l_2$	Number	Satisfies (5.4)
even	even	25	no
even	odd	16	yes
odd	even	20	yes
odd	odd	20	yes

TABLE 5.2

The table summarizes which entries of  $G_{AB}$  identically vanish because of the symmetries of the spherical harmonics under reflections through coordinate planes for all values of  $l$  and  $m$  with  $l \leq 2$ . (This is governed by equation (5.4).) Of the 81 possible matrix elements, only 25 have non-trivial values.

efficient implementation of the algorithm in general. It is also extremely useful in analyzing the algorithm in the context of the second topic of this section, explicit grid symmetries.

When evolving initial data with known symmetries, it is very common to evolve only that part of the data that is unique. In such cases, an appropriate symmetry boundary condition is applied at some edges of the grid. This is, however, inconvenient for wave extraction since computing spherical harmonic components (by any method) requires integrating over the full sphere. If data with octant symmetry, for example, is evolved only in a single octant, it is neither sufficient to apply the decomposition algorithm in that one octant nor to multiply the result of a single octant by 8 since the symmetry may forbid some modes as well as repeating them.

In principle the problem appears to be even more difficult for this particular decomposition method. Although the spherical harmonics have well defined symmetries under reflections, as summarized in Table 5.1, it is the adjoint harmonics that appear in (2.10). The adjoint harmonics, however, are constructed by contracting  $G^{AB}$  with the usual spherical harmonics, and this appears to mix different values of  $l$  and  $m$ . While this mixing does occur, the the matrix  $G_{AB}$  is sparse in just the right way to ensure that the adjoint harmonics have the same symmetries at the usual spherical harmonics.

A particular choice of the mapping  $(n, l, m) \mapsto A$  makes this easiest to see. Specifically, considering all values of  $l$  and  $m$  with  $l \leq 2$ , there is a basis in which  $G_{AB}$  takes block diagonal form

$$(G_{AB}) = \begin{pmatrix} \Xi_1 & & & \\ & \Xi_2 & & \\ & & \Xi_3 & \\ & & & \Xi_4 \end{pmatrix} \quad (5.5)$$

with all unwritten entries identically zero by symmetry. In this expression  $\Xi_1$  is a  $4N \times 4N$  matrix over the basis functions  $B_1 = \{Y_{n00}, Y_{n2,-2}, Y_{n20}, Y_{n22}\}$ ;  $\Xi_2$  is an  $N \times N$  matrix over the basis functions  $B_2 = \{Y_{n10}\}$ ;  $\Xi_3$  is a  $2N \times 2N$  matrix over the basis functions  $B_3 = \{Y_{n1,-1}, Y_{n11}\}$ ; and  $\Xi_4$  is a  $2N \times 2N$  matrix over the basis functions  $B_4 = \{Y_{n2,-1}, Y_{n21}\}$ . In this basis the matrix is block diagonal, so the inverse matrix

$$(G^{AB}) = \begin{pmatrix} \Xi_1^{-1} & & & \\ & \Xi_2^{-1} & & \\ & & \Xi_3^{-1} & \\ & & & \Xi_4^{-1} \end{pmatrix} \quad (5.6)$$



is also block diagonal and *the different basis sectors do not mix*. This last point is key. It implies that any particular adjoint harmonic is a linear combination of spherical harmonics from a single set  $B_k$

$$Y^{nlm} = \sum_{Y_{n'l'm'} \in B_k} (\Xi_k)^{(nlm)(n'l'm')} Y_{n'l'm'} \quad (5.7)$$

where  $k$  is the index such that  $Y_{nlm} \in B_k$ . Because, in each set  $B_k$ , the parity of  $l$  and the parity of  $m$  is the same on each  $Y_{nlm} \in B_k$ , and because, in light of Table 5.1, it is the parity of  $l$  and  $m$  that determines the symmetries of  $Y_{nlm}$  under reflections through planes, every spherical harmonic in  $B_k$  for any fixed  $k$  has the same symmetries under reflections as any other spherical harmonic in  $B_k$ . This implies that the adjoint harmonics also share this symmetry under reflection.

**6. Discussion.** In this paper I have provided detailed error estimates of the Misner algorithm for computing spherical harmonic components of data represented on a cubic grid. This analysis allows one, in principle, to chose the parameters of the algorithm such that its numerical errors scale any desired power of the grid spacing. The only limitation of this in practice is finding a scheme for approximating volume integrals on a shell of sufficiently high accuracy. (Misner's original choice allows for a second order accurate result.)

In addition, analysis of the symmetry properties of the spherical harmonics provides two insights: First, the number of operations required to initialize the data structures used to compute spherical harmonic components can be reduced by computing only those elements of  $G_{AB}$  that are not forbidden by symmetries, and, second, that the adjoint harmonics used by the algorithm have the same symmetries under reflections as the usual spherical harmonics. This second fact allows the method to be efficiently used on data with explicit grid symmetries when only the independent portion of that data is evolved.

**7. Acknowledgments.** I am grateful to Charles Misner, Richard Matzner, and John Baker for helpful discussions and suggestions. This work was supported by NASA Space Sciences grant ATP02-0043-0056. Portions of the text were written while the author held a National Research Council Post-doctoral Fellowship at NASA Goddard Space Flight Center.

#### REFERENCES

- [1] K. F. EVANS, *The spherical harmonics discrete ordinate method for three-dimensional atmospheric radiative transfer*, J. Atmos. Sci, 55 (1998), p. 429.
- [2] DAVID ROBERT FISKE, *Numerical studies of constraints and gravitational wave extraction in general relativity*, PhD thesis, University of Maryland, College Park, 2004. <http://hdl.handle.net/1903/1805>.
- [3] DAVID R. FISKE, JOHN G. BAKER, JAMES R. VAN METER, DAE-IL CHOI, AND JOAN M. CENTRELLA, *Wave zone extraction of gravitational radiation in three-dimensional numerical relativity*, Phys. Rev. D, 71 (2005), p. 104036.
- [4] J. N. GOLDBERG, A. J. MACFARLANE, E. T. NEWMAN, F. ROHRlich, AND E. C. G. SUDARSHAN, *Spin- $s$  spherical harmonics and  $\bar{\delta}$* , J. Math. Phys., 8 (1967), p. 2155.
- [5] JULIO A. KOVACS, PABLO CHACÓN, YAO CONG, ESSAM METWALLY, AND WILLY WRIGGERS, *Fast rotational matching of rigid bodies by fast Fourier transform acceleration of five degrees of freedom*, Acta Cryst. D, 59 (2003), p. 1371.
- [6] CHARLES W. MISNER, *Spherical harmonic decomposition on a cubic grid*, Class. Quant. Grav., 21 (2004), p. S243.
- [7] E. T. NEWMAN AND R. PENROSE, *Note on the Bondi-Metzner-Sachs group*, J. Math. Phys., 7 (1966), p. 863.

- [8] DANIEL R. SISSAN, NICOLÁS MUJICA, W. ANDREW TILLOTSON, YI-MIN HUANG, WILLIAM DORLAND, ADIL B. HASSAM, THOMAS M. ANTONSEN, AND DANIEL P. LATHROP, *Experimental observation and characterization of the magnetorotational instability*, Phys. Rev. Lett., 93 (2004), p. 114502.
- [9] D. STAMMER, R. TOKMAKIAN, A. SEMTNER, AND C. WUNACH, *How well does a 1/4 degree global circulation model simulate large-scale oceanic observations?*, J. Geophys. Res., 101 (1996), p. 25779.
- [10] WALDO TOBLER, *Preliminary representation of world population by spherical harmonics*, Proc. Natl. Acad. Sci. USA, 89 (1992), p. 6262.
- [11] D. R. WEIMER, *Models of high-altitude electric potentials derived with a least error fit of spherical harmonic coefficients*, J. Geophys. Res., (1995), p. 19595.
- [12] WILLY WRIGGERS AND PABLO CHACÓN, *Modeling tricks and fitting techniques for multiresolution structures*, Structure, 9 (2001), p. 779.